

# Fabrication and Performance of InP-Based Heterostructure Barrier Varactors in a 250-GHz Waveguide Tripler

Xavier Mélique, Alain Maestrini, Robert Farré, Patrick Mounaix, Michel Favreau, Olivier Vanbésien, Jean-Marc Goutoule, Francis Mollot, Gérard Beaudin, *Senior Member, IEEE*, Tapani Närhi, *Member, IEEE*, and Didier Lippens

**Abstract**—High-performance InGaAs/InAlAs/AlAs heterostructure barrier varactors (HBV's) have been designed, fabricated, and RF tested in a 250-GHz tripler block. The devices with two barriers stacked on the same epitaxy are planar integrated with coaxial-, coplanar-, and strip-type configurations. They exhibit state-of-the-art capacitance voltage characteristics with a zero-bias capacitance  $C_j^0$  of  $1 \text{ fF}/\mu\text{m}^2$  and a capacitance ratio of 6 : 1. Experiments in a waveguide tripler mount show a 9.8-dBm (9.55-mW) output power for 10.7% conversion efficiency at 247.5 GHz. This is the highest output power and efficiency reported from an HBV device at J-band (220–325 GHz).

**Index Terms**—Harmonic multipliers, heterostructure barrier varactors, millimeter waves.

## I. INTRODUCTION

HETERODYNE receivers are used for high spectral resolution radioastronomy and earth remote sensing. The local oscillator is one of the key components in heterodyne receivers, and harmonic multipliers using varactors are being developed to meet the local-oscillator requirement for future millimeter- and submillimeter-wave space applications. In this context, novel varactor structures, used as the nonlinear devices in the multipliers, and new integration techniques are being investigated. The heterostructure barrier varactor (HBV) proposed in 1989 by Rydberg and Kollberg [1] is one promising candidate for space terahertz applications. It exhibits a sharp nonlinearity and a symmetrical capacitance–voltage ( $C$ – $V$ ) curve around the 0-V bias point. Such a natural symmetry greatly simplifies the multiplier design and opens the way for higher harmonic operating modes.

Manuscript received March 9, 1999. This work was supported by the European Space Agency under Contract 9777/92/NL/PB.

X. Mélique, P. Mounaix, O. Vanbésien, F. Mollot, and D. Lippens are with the Institut d'Electronique et de Microélectronique du Nord, Université des Sciences et Technologies de Lille, 59652 Villeneuve d'Ascq Cedex, France (e-mail: Didier.Lippens@IEMN.univ-Lille1.fr).

A. Maestrini was with the Département d'Études pour la Matière Interstellaire en Infrarouge et en Millimétrique, Observatoire de Paris Meudon, 75014 Paris, France. He is now with the Jet Propulsion Laboratory, Pasadena, CA 91109 USA.

R. Farré, M. Favreau, and J.-M. Goutoule are with the Instrumentation et Micro-ondes Département, Matra Marconi Space, 31077 Toulouse Cedex, France.

G. Beaudin is with the Département d'Études pour la Matière Interstellaire en Infrarouge et en Millimétrique, Observatoire de Paris Meudon, 75014 Paris, France.

T. Närhi is with the Payload Systems Division, European Space Research and Technology Center, 2000 AG Noordwijk, The Netherlands.

Publisher Item Identifier S 0018-9480(00)04663-9.

Since the pioneering work of the Chalmers group [1], [2] on HBV's achieving 2 mW and 5% efficiency from 210 to 280 GHz with a whisker technology [2], much work has been devoted to this new kind of device, which has shown promise at millimeter wavelengths. A 200-GHz tripler using a whisker-contacted single-barrier GaAs varactor with an overall efficiency of 2% was demonstrated at the Jet Propulsion Laboratory, Pasadena, CA [3]. A 10- $\mu\text{m}$ -diameter device yielded a delivered output power of 3.6 mW (2.5% conversion efficiency) at 234 GHz using AlGaAs/GaAs heterostructures [4] showing self-heating effects. Recently, we reported, in collaboration with the Rutherford Appleton Laboratory, Didcot, U.K., efficiency of 5% and output power of 5 mW at 216 GHz [5] with no saturation effects for InP-based devices fabricated at the Institut d'Electronique et de Microélectronique du Nord (IEMN), Villeneuve d'Ascq, France. Also, high performances have been published at W-band (75–110 GHz) with 19.6-dBm output power at 93 GHz using a ten-stack device with 22-V breakdown voltage [6].

In this paper, we report on the design, fabrication, and RF testing in a 250-GHz waveguide tripler of high-quality HBV's having a step-like barrier scheme. Two barriers are sequentially grown by molecular beam epitaxy, yielding an overall breakdown voltage of 12 V. Various device layouts have been developed, including a coaxial type for rapid assessment, a coplanar type for deriving a small-signal lumped-element equivalent circuit, and a strip type for tripler experiments. The fabricated devices achieve a capacitance ratio of 6 : 1 for a zero-bias capacitance of  $1 \text{ fF}/\mu\text{m}^2$ . Experiments in a waveguide tripler block show a delivered output power of about 10 mW (10% efficiency) at 247.5 GHz. To our knowledge, these results are record performances with respect to the delivered power and conversion efficiency reported in the literature for HBV's [1]–[11].

## II. DEVICE DESIGN AND FABRICATION

Fig. 1 shows the epitaxial material grown at IEMN by gas source molecular beam epitaxy starting from a semiinsulating Fe-doped InP substrate. Two basic  $\text{In}_{0.53}\text{Ga}_{0.47}\text{As}/\text{In}_{0.52}\text{Al}_{0.48}\text{As}/\text{AlAs}/\text{In}_{0.52}\text{Al}_{0.48}\text{As}/\text{In}_{0.53}\text{Ga}_{0.47}\text{As}$  schemes were series integrated during the same epitaxy. Previously, it was found that the device characteristics scale with epilayer complexity. Therefore, the voltage breakdown should be twice that of the single barrier device, whereas the

X 2	InGaAs	$5 \times 10^{18} \text{ cm}^{-3}$	500nm
	InGaAs	$1 \times 10^{17} \text{ cm}^{-3}$	300nm
	InGaAs	Undoped	5nm
	InAlAs	Undoped	5nm
	AlAs	Undoped	3nm
	InAlAs	Undoped	5nm
	InGaAs	Undoped	5nm
	InGaAs	$1 \times 10^{17} \text{ cm}^{-3}$	300nm
	InGaAs	$5 \times 10^{18} \text{ cm}^{-3}$	500nm
	InP Substrate		

Fig. 1. Epitaxial sequence for the devices grown by gas source molecular beam epitaxy. Two barriers were systematically series integrated during epitaxy.

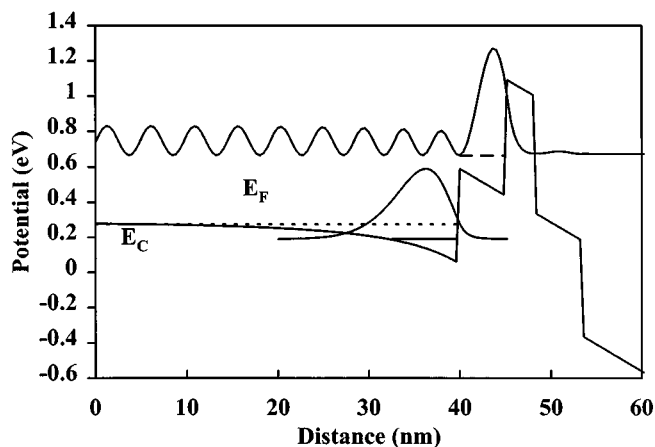


Fig. 2. Illustration of design rules making use of bandgap engineering by a plot of conduction band edge versus distance. The capacitance nonlinearity is due to the electron accumulation in the triangular quantum well, which forms at low energy on the left-hand side. The leakage current results from a resonant tunneling process activated at higher energy.

capacitance is half the value for one barrier [12]. The design of epilayers was carried out by means of an in-house Schrödinger and Poisson equations solver. For a given epilayer sequence, whatever the degree of complexity, this code computes the band-bending profile along with the electron wave function. The main goal of the bandgap engineering, developed in this paper, was to drastically reduce the leakage current [13] by the use of a three-layered blocking barrier. On the other hand, the capacitance of the device was optimized by a careful analysis of the positive and negative charges stored on each side of the heterostructure.

Fig. 2 illustrates both the conduction and storage mechanisms at a bias voltage of 4 V for a single barrier device, having the growth parameters listed in Fig. 1, with the plot of the conduction band edge as a function of distance. An accumulation forms in front of the heterostructure barrier in a quasi-triangular quantum well. A computation of the sheet carrier density  $n_s$  via

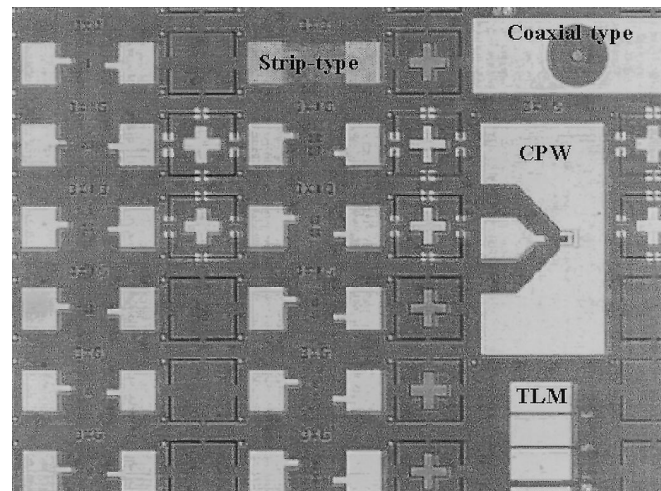


Fig. 3. Plan view of the mask set before air-bridge implementation. The layout includes coaxial-, coplanar-, and series- type configurations along with TLM patterns.

the electron wave function as a function of voltage is a direct calculation (after derivating  $n_s$  with respect to voltage) of the expected  $C$ - $V$  characteristics.

For illustration of conduction mechanisms, we have also plotted the wave function corresponding to the resonant tunneling process demonstrated in [14]. This tunneling process is responsible for the leakage current, which is found to be very low at moderate voltages. In contrast, the breakdown around 6 V for a single barrier device is due to impact ionization. It is worth noting that the characteristic tunneling energy is several hundred millielectron volts ( $>600 \text{ meV}$ ) and, hence, is much higher than the relevant energy value involved in a GaAs technology. For instance, the relevant characteristic energy would be about 180 meV for a GaAs/ $\text{Al}_{0.7}\text{Ga}_{0.3}\text{As}$ /GaAs. This is the basic reason why the voltage handling of the diodes is dramatically improved and alleviates self-heating effects. In practice, an improvement of a factor of three is found (6 V instead of 2 V).

In addition to the careful design of the blocking barrier, special attention was also paid to the adjacent layer that greatly influences the tradeoff between current saturation effects [15] and achievable capacitance ratio. The former can be overcome by increasing the doping concentration. The latter is related in first approximation to the ratio between the barrier thickness (the screening length also has to be taken into account for a better estimate) and the depletion layer thickness.

Fig. 3 is an optical view of the layout prior to the implementation of the air bridges. Three kinds of devices have been patterned on the mask set. The simplest is a coaxial type. It consists of a mesa-etched circular-shaped device with a concentric ring-shaped side contact. It is used for rapid assessments of current-voltage and  $C$ - $V$  characteristics without the requirement of an air-bridge contacting technology [16], [17]. For on-wafer characterization, the RF probes are positioned directly on top of the device.

The second test configuration is of coplanar type [coplanar waveguide (CPW)]. This microwave compatible technology permits us to characterize small-area devices interconnected to

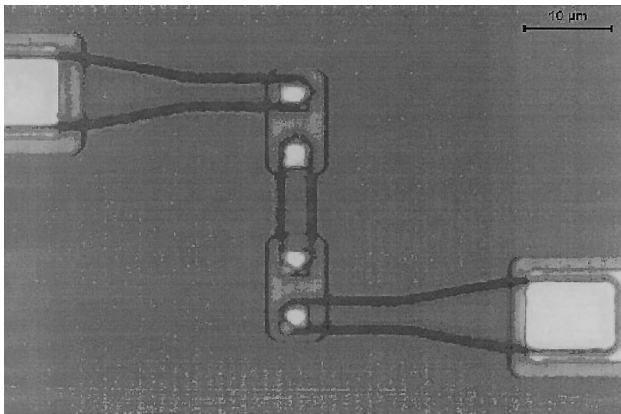


Fig. 4. Planar integration of four dual heterostructure barriers in series prior to the implementation of metallization of the air bridges. Here, the overall number of equivalent barriers is eight (two by epitaxy and four by planar integration).

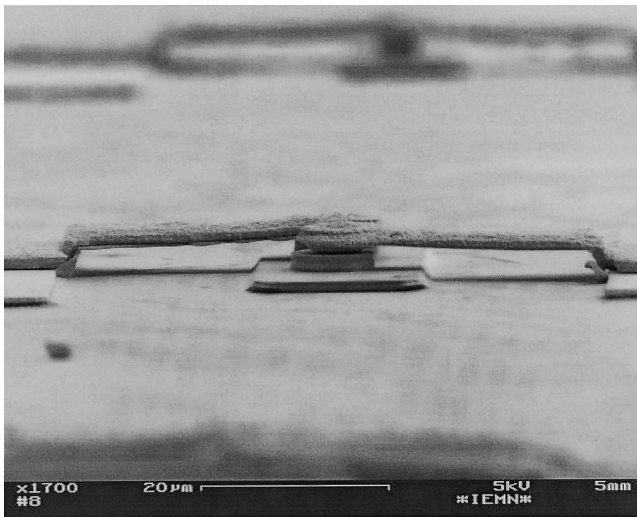


Fig. 5. Close-up view of a typical device epitaxially (two barriers) and planar integrated (two interconnected devices). Hence, the number of equivalent barriers is four.

the CPW line by means of an air bridge. The third test scheme, labeled strip type, consists of two pads facing each other. Fig. 4 illustrates this scheme by means of an optical view of a planar integrated device prior to the air-bridge metallization. Here, the overall number of barrier is eight (two barriers were epitaxially integrated for four air-bridged devices). Also, several devices with areas ranging from 10 to 100  $\mu\text{m}^2$  have been written on the mask set in order to test the devices at different frequencies. Finally, the layout includes a transmission-line method (TLM) pattern for assessing the quality of the ohmic contact.

Fig. 5 is a scanning electron microphotograph (SEM) of a planar integrated device equivalent to four barriers (two were integrated during epitaxy and two by means of air bridges). The technological effort was mainly concentrated on the mesa etching by means of reactive ion etching (RIE) in order to avoid undercutting effects and on the fabrication of self-sustaining metallic bridges for interconnecting the top ohmic contacts to the pads. Also, for a good definition, the writing steps were performed by electron beam (LEICA High-Resolution

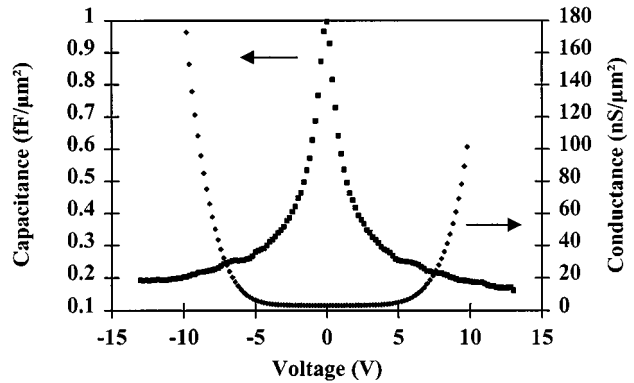


Fig. 6. Small-signal conductance and capacitance versus voltage measured at 300 K with the coaxial test pattern. The measurement frequency is 500 MHz for the  $C$ - $V$  curve.

Electron-Beam Pattern Generator). Otherwise, conventional fabrication technologies were employed with sequential Ni/Ge/Au/Ti/Au overlay for the ohmic contact fabrication and  $\text{H}_3\text{PO}_4/\text{H}_2\text{O}_2/\text{H}_2\text{O}$  solution for the wet etching of isolation mesa taking advantage of the high selectivity between InGaAs and InP. For the metallization of the air bridges, we employed either electroplating technique (as is the case in Fig. 5) or evaporation procedure (see [5, Fig. 1]). For the latter, we developed a pyrolyzation technique of photo resists, which results in a convex-shaped temporary mold for thin metal film evaporation.

### III. SMALL-SIGNAL MEASUREMENTS

The RF measurements of the devices were carried out in two stages: on-wafer probing and measurements on discrete devices. As demonstrated in our previous work [16], the intrinsic nonlinear  $C$ - $V$  characteristics can be measured without deembedding techniques across the whole frequency range up to 110 GHz. Fig. 6 displays the result achieved in the last technological run for two barriers in series corresponding to a dual heterostructure barrier varactor (DHBV). The symmetry in the  $C$ - $V$  characteristic is excellent. This is a welcome feature for efficiently rejecting the even harmonics as seen in the following. The intrinsic zero-bias voltage is 1  $\text{fF}/\mu\text{m}^2$ . This normalization to the area can be performed since this nonlinear term is dominated by a one-dimensional depletion effect. The capacitance ratio, measured at zero bias and just before breakdown, is 6 : 1 and is slightly higher than our previously published value (5 : 1). Also plotted in Fig. 6 is the voltage dependence of the conductance of the device. Note the unit of the conductance in  $\text{nS}/\mu\text{m}^2$ . Thus, the voltage handling of such a device is remarkable with a “safe” operating voltage range at least of 20-V peak-to-peak. The conductance curve is slightly asymmetrical, but this asymmetry has no consequence on the device performance under zero-bias condition. In fact, the leakage current is so small that it does not influence the overall performance of devices. Moreover, the fact that this asymmetry is not very pronounced demonstrates the high quality of the samples since the leakage current is due to a tunneling process that is known to be strongly dependent on the barrier quality. Also, it is worth mentioning that this kind

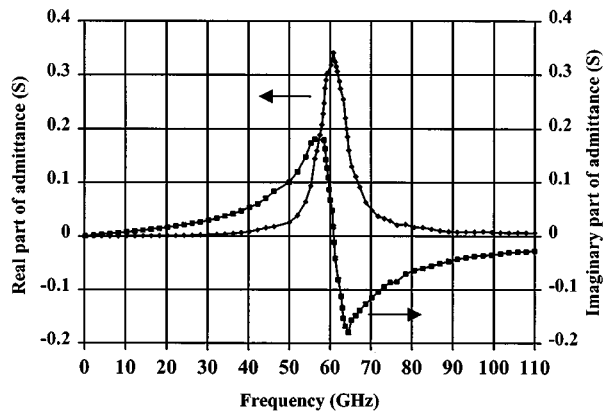


Fig. 7. Small-signal impedance of air-bridged devices as a function of frequency at zero bias achieved by means of scattering-parameter measurements.

of experiment gives some estimate of the series resistance. Previous works showed that the spreading dominates for the present topology and area range. An analysis of the series impedance of planar diodes can be found in [18]. Experimentally, we measured a few ohms, the exact value depending on the area, despite the fact that large anode contacts were used. TLM measurements by means of a pattern of rectangular pads with increasing spacing for varying the overall resistance (Fig. 2) were performed yielding a resistivity of typically  $1 \times 10^{-7} \Omega \text{ cm}^2$ , showing the benefits of the low bandgap of InGaAs contacting layer and of the high doping concentration ( $\sim 5 \times 10^{18} \text{ cm}^{-3}$ ). This means that the contact resistance is less than  $1 \Omega$  for an area greater than  $10 \mu\text{m}^2$ .

Fig. 7 shows the frequency dependence of the real and imaginary parts of impedance of an air-bridge contacted diode measured from dc to 110 GHz. The self-inductance due to interconnecting elements gives rise to a well-defined resonance effect; here, at  $\sim 60$  GHz for a  $60\text{-}\mu\text{m}^2$  device. This resonance is particularly useful for fitting a lumped-element equivalent circuit, to be used in the subsequent harmonic-balance analysis [19]. Confidence in the accuracy of measurement can also be found by full electromagnetic analysis of the CPW circuit and connecting elements [20]. In contrast, we deduced the series resistance by fitting the frequency dependence of diode impedance using a lumped-element approach. The series resistance is a key parameter for achieving high cutoff frequency ( $f_c = (S_{\text{max}} - S_{\text{min}})/2\pi R_s$ , where the elastances are  $S_{\text{max}} = 1/C_{\text{min}}$  and  $S_{\text{min}} = 1/C_{\text{max}}$ ) and, hence, high performance. We found  $R_s = 3.8 \Omega$  for a  $30\text{-}\mu\text{m}^2$ ,  $2.5 \Omega$  for  $60\text{-}\mu\text{m}^2$ , and  $2.2 \Omega$  for a  $121\text{-}\mu\text{m}^2$  device. One can note that the series resistance does not scale with area as expected when the spreading resistance plays the major role. From the data extracted from both types of measurements (coaxial and CPW types), an estimate of the cutoff frequency of the diodes can be obtained. We thus calculate  $f_c = 1.5$  THz and  $2.1$  THz, respectively, for double-barrier heterostructures (DBH's) of  $60$  and  $30 \mu\text{m}^2$  from the small-signal measurements. For large-signal measurements, the devices were mounted in a waveguide multiplier block, and the results are reported hereafter.

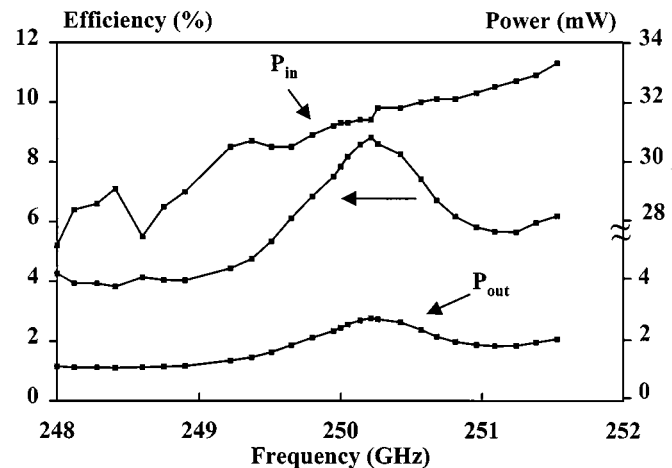


Fig. 8. Input and output power along with conversion efficiency versus frequency. The diode diameter is  $6 \mu\text{m}$ . The number of barriers is four. The input frequencies corresponding to this band are  $82.66$  and  $84$  GHz, respectively.

#### IV. TRIPLER MEASUREMENTS

The multiplier block used for the tripler measurements at  $250$  GHz is a crossed waveguide-type mount with a design basically similar to Archer's [21] with waveguides coupled through a low-pass stripline filter. The pump power incident in the full-height WR-8 waveguide is fed to the planar integrated diode through a stripline  $E$ -plane transition and through the low-pass filter implemented on a  $100\text{-}\mu\text{m}$ -thick quartz substrate. Impedance matching at the pump power is achieved using two sliding noncontacting backshorts. The output was also equipped with two backshorts. On the other hand, the multiplier block differs from that of Archer's tripler design by the full-height output waveguide [22] where the diode chip is mounted in a flip-chip technology using a conductive epoxy. To this aim, the diode samples were first lapped to a thickness of about  $100 \mu\text{m}$  by an HCl wet etching and then diced into discrete devices. The overall chip dimensions are  $100 \times 220 \times 100 \mu\text{m}^3$ .

In the first experiments, the moderate input power was taken from a Gunn oscillator, which can be mechanically tuned. Input power was measured with a recently calibrated HP power head, whereas the output power was recorded using an Anritsu power head, which has been calibrated with a Thomas Keating power meter. Fig. 8 shows the variation in the  $248\text{--}251.5$ -GHz range of input power, output power, and efficiency. These measurements were carried out with a DBH with two  $6\text{-}\mu\text{m}$ -diameter diodes planar integrated and fixed tuning of backshorts. A rather smooth resonance can be noted with a peak efficiency of approximately  $8.5\%$ . For experiments at higher power levels up to  $P_{\text{in}} = 100$  mW, we used a carcinotron (Thomson, serial number C040), which can deliver much higher power in the  $77\text{--}82.5$ -GHz range, but has power jumps in the frequency response. Fig. 9 shows the output power and conversion efficiency as a function of input power for an output frequency of  $247.5$  GHz. The maximum efficiency was obtained with about  $60\text{-mW}$  input power. The efficiency variations around this maximum are relatively flat.

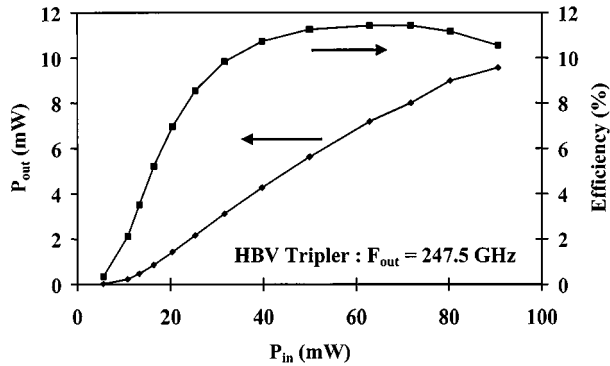


Fig. 9. Output power and conversion efficiency as a function of input power. Same device parameters as before. Here, the input power was supplied by a carcinotron.

The maximum output power was 9.8 dBm (9.55mW) and was obtained with an efficiency of 10.7%.

In comparison to our previous experiment with  $2 \times 12 \mu\text{m}^2$  samples [5], an increase in efficiency by as much as 11.5% has been achieved. It is believed that we took advantage of smaller area devices that can be more easily driven into non-linear regime. The output waveguide was WR 4, and this permitted us to measure the second harmonic content, which was found to be  $-25$  dB below the third harmonic. This very good rejection of the even harmonic is a direct consequence of the excellent symmetry in the  $C$ - $V$  characteristics. At short term, it is believed that this very good performances with simultaneously high output power and efficiency can be further improved in the future.

## V. CONCLUSIONS

Record performances with a simultaneous efficiency in excess of 10% and an output power around 10 dBm have been demonstrated in a 250-GHz tripler experiment. To realize this, high-quality InP-based HBV's have been designed and fabricated in stacked and planar integrated configurations. Small-signal measurements shows high-capacitance ratio (in excess of 5 : 1), low series resistance of a few ohms, and promising voltage handling capability of the order of a 10-V peak. Further improvements in the frequency and power capabilities of the devices should be achieved in the short term by the fabrication of lower capacitance devices, including liftoff and transferred techniques [23] on quartz and/or monolithic integration on semiconductor membranes.

## ACKNOWLEDGMENT

The authors thank E. Delos, S. Lepilliet, and D. Vandermoere, IEMN, Lille, France, for their technical assistance. The authors would also like to express their deep appreciation to P. Goy, Ecole Normale Supérieure, Paris, France, for his key role in the experiment, and E. Kollberg, J. Stake, and L. Dillner, Chalmers University of Technology, Göteborg, Sweden, for their fruitful discussions.

## REFERENCES

- [1] E. Kollberg and A. Rydberg, "Quantum-barrier-varactor diodes for high-efficiency millimeter wave multipliers," *Electron. Lett.*, vol. 25, pp. 1696–1697, Dec. 1989.
- [2] A. Rydberg, H. Grönqvist, and E. Kollberg, "Millimeter- and sub-millimeter-wave multipliers using quantum barrier-varactor (QBV) diodes," *IEEE Electron Device Lett.*, vol. 11, pp. 373–375, Sept. 1990.
- [3] D. Choudhury, M. A. Frerking, and P. D. Batelaan, "A 200-GHz tripler using a single barrier varactor," *IEEE Trans. Microwave Theory Tech.*, vol. 41, pp. 595–599, Apr. 1993.
- [4] J. Stake, L. Dillner, S. H. Jones, C. M. Mann, J. Thornton, J. R. Jones, W. L. Bishop, and E. Kollbert, "Effects of self heating on planar heterostructure barrier varactor diodes," *IEEE Trans. Electron Devices*, vol. 45, pp. 179–182, Nov. 1998.
- [5] X. Mélique, C. Mann, P. Mounaix, J. Thornton, O. Vanbésien, F. Mollot, and D. Lippens, "5-mW and 5% efficiency 216 GHz InP-based heterostructure barrier varactor tripler," *IEEE Microwave Guided Wave Lett.*, vol. 8, pp. 384–386, Nov. 1998.
- [6] A. Rahal, R. G. Bosisio, C. Rogers, J. Ovey, M. Sawan, and M. Missous, "A  $W$ -band medium power multistack quantum barrier varactor frequency multiplier," *IEEE Microwave Guided Wave Lett.*, vol. 5, pp. 368–370, Nov. 1995.
- [7] J. R. Jones, W. L. Bishop, S. H. Jones, and G. B. Tait, "Planar multibarrier 80/240-GHz heterostructure barrier varactor triplers," *IEEE Trans. Microwave Theory Tech.*, vol. 45, pp. 512–518, Apr. 1997.
- [8] K. Krishnamurthi, S. M. Nilsen, and R. G. Harrison, "GaAs Single-barrier varactors for millimeter-wave triplers: Guidelines for enhanced performances," *IEEE Trans. Theory Tech.*, vol. 42, pp. 2512–2516, Dec. 1994.
- [9] A. Rahal, E. Boch, C. Rogers, J. Ovey, and R. G. Bosisio, "Planar multistack quantum barrier varactor tripler evaluation at  $W$ -band," *Electron. Lett.*, vol. 31, pp. 2022–2023, 1995.
- [10] K. Krishnamurthi and R. G. Harrison, "Millimeter-wave frequency tripling using stacked heterostructure barrier varactor on InP," in *IEEE Proc. Microwave Antennas Propagat.*, vol. 143, Aug. 1996, pp. 272–276.
- [11] A. V. Räisänen, T. J. Tolmunen, M. Natzi, M. A. Frerking, E. Brown, H. Grönqvist, and S. M. Nilsen, "A single barrier quintupler at 170 GHz," *IEEE Trans. Microwave Theory Tech.*, vol. 43, pp. 685–688, Mar. 1995.
- [12] E. Lheurette, P. Mounaix, P. Salzenstein, F. Mollot, and D. Lippens, "High performance InP-based heterostructure barrier varactor in single and stack configuration," *Electron. Lett.*, vol. 32, pp. 1417–1418, July 1996.
- [13] V. K. Reddy and D. P. Neikirk, "High breakdown voltage AlAs/InGaAs quantum barrier varactor diodes," *Electron. Lett.*, vol. 29, pp. 465–466, Mar. 1993.
- [14] R. Havart, E. Lheurette, O. Vanbésien, P. Mounaix, F. Mollot, and D. Lippens, "Step-like heterostructure barrier varactor," *IEEE Trans. Electron Devices*, vol. 45, pp. 2291–2297, Nov. 1998.
- [15] E. Kollberg, T. J. Tolmunen, M. A. Frerking, and J. East, "Current saturation in submillimeter wave varactors," *IEEE Trans. Microwave Theory Tech.*, vol. 40, pp. 831–838, 1992.
- [16] E. Lheurette, X. Mélique, P. Mounaix, F. Mollot, O. Vanbésien, and D. Lippens, "Capacitance engineering for InP-based heterostructure barrier varactor," *IEEE Electron Device Lett.*, vol. 19, pp. 338–340, Sept. 1998.
- [17] V. Duez, X. Mélique, O. Vanbésien, P. Mounaix, F. Mollot, and D. Lippens, "High capacitance ratio with GaAs/InGaAs/AlAs heterostructure quantum well-barrier varactors," *Electron. Lett.*, vol. 34, pp. 1860–1861, Sept. 1998.
- [18] B. Gemont and M. Shur, "Spreading resistance of around ohmic contact," *Solid State Electron.*, vol. 36, pp. 143–146, 1993.
- [19] J. Carbonell, R. Havart, X. Mélique, P. Mounaix, O. Vanbésien, J. M. Goutoule, and D. Lippens, "Reverse engineering through electromagnetic and harmonic balance simulations," in *Proc. European Microwave Conf.*, Amsterdam, The Netherlands, Oct. 1998, pp. 123–128.
- [20] X. Mélique, J. Carbonell, R. Havart, P. Mounaix, O. Vanbésien, and D. Lippens, "InGaAs/InAlAs/AlAs heterostructure barrier varactors for harmonic multiplication," *IEEE Microwave Guided Wave Lett.*, vol. 8, pp. 254–256, July 1998.
- [21] J. Archer, "An efficient 200–290 GHz frequency tripler incorporating a novel stripline structure," *IEEE Trans. Microwave Theory Tech.*, vol. MTT-32, pp. 416–420, Apr. 1984.
- [22] L. Dillner and E. Kollberg, private communication.
- [23] S. Arscott, P. Mounaix, and D. Lippens, "Transferred InP-based HBV's on glass substrate," *Electron. Lett.*, vol. 35, no. 17, pp. 1493–1494, Aug. 1999.



**Xavier Mélique** was born in Tourcoing, France, on April 12, 1972. He received the M.S. and Ph.D. degrees from the University of Lille, Lille, France, in 1994 and 1999, respectively.

He is currently with the Institut d'Electronique de Microelectronique du Nord (IEMN), Villeneuve d'Ascq, France, where he is involved with the technological planar integration of a high-performance HBV multiplier aimed at operating at terahertz frequency. His current interest concerns nonlinear transmission lines periodically loaded by HBV devices for operation at millimeter wavelengths for telecommunications.



**Alain Maestrini** was born in Marseille, France, in 1970. He received the engineer diploma from the National Graduate School of Telecommunications of Brittany, ENST de Bretagne, Bretagne, France, in 1993, and the Ph.D. degree from the Département d'Études pour la Matière Interstellaire en Infrarouge et en Millimétrique (DEMIRM), Paris, France, in 1999.

Following two years as an Engineer in the Receiver Group of the IRAM 30-m telescope, Institut di RadioAstronomie Millimétrique, Granada, Spain, he joined the Observatory of Paris, DEMIRM, Paris, France, in planar-diode millimeter-wave multipliers. In July 1999, he joined the Sub-Millimeter-Wave Advanced Technology Group, NASA Jet Propulsion Laboratory, Pasadena, CA, as a Post-Doctoral Researcher. His current interest concerns the development of multipliers circuits for the FIRST project.



**Robert Farré** was born in Perpignan, France, in 1968. He received the degree in technology of microwave from the Institut Universitaire de Technologie (IUT) Ville d'Avray, near Paris, France, in 1990, and the Master's degree in electronics from the Conservatoire National des Arts et Métiers (CNAM) of Paris, Paris, France, in 1993.

From 1991 to 1994, he was with the Laboratoire Central Thomson d'Application Radar (formerly the Laboratoire Central des Télécommunications), Vélizy, near Paris, France. Since 1994, he has been with Matra Marconi Space (MMS), Toulouse, France, where he is currently involved with the microwave and millimeter wave project for responsible alignment and test of components such as mixers, frequency multipliers, noise amplifiers, and elements of quasi-optical demultiplexing networks.



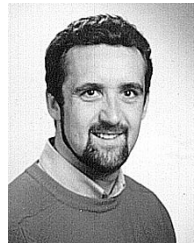
**Patrick Mounaix** was born in Latresne, France, in 1964. He received the degree of engineer of material science from the Ecole Universitaire D'Ingénieur de Lille (EUDIL), Lille, France, in 1988, and the Ph.D. degree on quantum devices in dipole and tripole configuration from the University of Lille, Lille, France, in 1992.

He then became a Chargé de Recherches at the Centre National de la Recherche Scientifique (CNRS), High-Frequency Development, Institut d'Electronique et de Microélectronique du Nord (IEMN), Villeneuve d'Ascq, France, as part of the Quantum Device Group. He is currently interested in various projects such as simulation and characterization of quantum devices, development of low parasitic technology for millimeter- and submillimeter-wave components, and microtechnologies and microsystems on III-V materials.



**Michel Favreau** was born in Clermont Ferrand, France, in 1966. He received the Engineer degrees in electricity from the l'École Nationale Supérieure d'Electricité, Gif sur Yvette, France, in 1989.

He was involved in 100–500-MHz radar design at Centre d'Etudes Nucléaires (CEA), Saclay, France. In 1990, he joined Matra Marconi Space, Toulouse, France, where he has designed frequency-selective surfaces and complete quasi-optical demultiplexers at 89/190 GHz for space-borne millimeter-wave radiometers. From 1993 to 1995, he designed frequency-selective surfaces (FSS's), frequency multipliers, and mixers from 23 to 190 GHz. Since 1995, he has designed and developed a 500-GHz receiver, including mixers and FSS's.



**Olivier Vanbésien** was born in Armentières, France, on November 11, 1964. He received the Engineer degree from the Institut Supérieur d'Electronique du Nord (ISEN), Lille, France, in 1987, and the Ph.D. degree in quantum devices from the University of Lille, Lille, France, in 1991.

He joined the High Frequency Department, Institut d'Electronique et de Microélectronique du Nord (IEMN), Villeneuve d'Ascq, France, as a Chargé de Recherches at the Centre National de la Recherche Scientifique (CNRS), Paris, France, as part of the Quantum Device Group. His current interest concerns the simulation and characterization of intraband and interband resonant tunneling diodes, as well as quantum waveguide-based structures and their optimization for operation at millimeter and submillimeter wavelengths. He recently began working on photonic crystals for application in the terahertz frequency range.



**Jean-Marc Goutoule** was born in Toulouse, France, in 1953. He received the Engineer degree in electronics from the l'École Nationale Supérieure D'Électronique, Hydraulique, Informatique de Toulouse, France, and the Doctor Engineer degree from the Ecole Nationale d'Aeronautique et de l'Espace, Toulouse, France.

From 1979 to 1981, he was with Thomson, where he was involved with advanced devices using fin line, coplanar lines, and ferrite planar lines. In 1981, he joined Alcatel Espace, where he developed receivers for space telecommunications, up to 30 GHz. Since 1988, he has been in charge of Matra Marconi Space, Toulouse, France, where he is involved with millimeter-wave device research and space-borne radiometer design up to 500 GHz.



**Francis Mollot** was born in Courbevoie, France, on November 1, 1946. He received the Engineer degree from INSA-Toulouse, Toulouse, France, in 1968, and the Docteur es Sciences degree for his work on the metastable optical properties of amorphous chalcogenide semiconductors from Université Paris 7, Paris, France, in 1979.

He was with the Groupe de Physique des Solides, l'École Nationale Supérieure (ENS), Paris, France. He participated in the creation of the L2M-CNRS Bagnex Laboratory in 1984, where he began an activity in molecular beam epitaxy and physics of III-V semiconductor heterostructures and GaAs-AlAs superlattices. In 1990, he was with Alcatel Alstom Research, Mercoussis, France, where he was involved with quantum effects for optical modulation for fiber communications. Since 1992, he has been Directeur de Recherches, Centre National de la Recherche Scientifique (CNRS), Institut d'Electronique et de Microélectronique du Nord (IEMN), Villeneuve d'Ascq, France, where he is currently in charge of gas source molecular beam epitaxy and physical studies on quantum semiconductor heterostructures. He is concerned with bandgap engineering and growth of structures on InP or GaAs, phosphide-arsenide interfaces, and joint use of phosphorous and aluminum for large-band offsets.



**Gérard Beaudin** (SM'91) was born in 1946. He received the Ph.D. degree in physics from the University of Paris-Orsay, Paris, France, in 1972.

He is currently the Senior Research Engineer Manager of the Microwave Laboratory, Département d'Études pour la Matière Interstellaire en Infrarouge et en Millimétrique en Infrarouge et en Millimétrique (DEMIRM). He developed decimeter and centimeter low-noise heterodyne receivers for the Nançay Radioastronomy station from 1966 to 1972. Since 1973, he has been in charge of research and technology developments and the (sub)millimeter heterodyne instrumentation for application to remote sensing, aeronomy, and meteorology (ground stations, stratospheric balloon bornes, space bornes). He has contributed to over 50 papers and conferences.

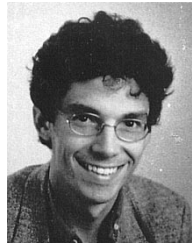
Dr. Beaudin is a senior member of the Société des Electriciens et Electroniciens (SEE) and the Société Française de Physique (SFP). He is vice-president of the CNFRS Radioastronomy Group of the International Scientific Radio Union (URSI). He was the recipient of the 1998 Award of the French Physics Science Society. He received the 1980 prize from the French Academy of Sciences for detection of Rydberg atoms emission in the millimeter wavelength at ENS. He received another prize for his work in applied science in 1990.



**Tapani Närhi** (S'78–M'80) received the M.Sc. and D.Tech. degrees in electrical engineering from the Helsinki University of Technology, Espoo, Finland, in 1978 and 1993, respectively.

From 1978 to 1981, he was a Research Engineer at the Telecommunications Laboratory, Technical Research Centre of Finland (VTT), where he was involved in the design and characterization of solid-state microwave circuits. From 1981 to 1984, he was a Communications Engineering Instructor at the Civil Aviation Training Centre, Dhaka, Bangladesh, for the International Civil Aviation Organization (ICAO). After returning to VTT in 1984, he was a Project Manager in several research and development projects dealing with communications applications of microwave technology, concentrating on mobile communications. In 1990, he was with the European Space Agency (ESA). Since then, he has been involved with space applications of microwave and millimeter-wave technology at the Payload Systems Division, European Space Research and Technology Center (ESTEC), Noordwijk, The Netherlands. His research interests include linear and nonlinear microwave and millimeter-wave circuits and computer-aided design (CAD) methods.

Dr. Närhi was the recipient of the 1998 Microwave Prize.



**Didier Lippens** was born in Lille, France, in 1952. He received the Ph.D. degree and the Doctorat ès Sciences Physiques degree from the University of Lille, Lille, France, in 1978 and 1984, respectively.

From 1979 to 1980, he was an Engineer at Thomson Laboratories, Paris, France. From 1981 to 1987, he was a Chargé de Recherches for the Centre National de la Recherche Scientifique (CNRS), Centre Hyperfréquences et Semiconducteurs. Since 1990, he has been Directeur de Recherches and Professor at the Institut d'Électronique et de

Microélectronique du Nord (IEMN), Université des Sciences et Technologies de Lille, Villeneuve d'Ascq, France. For the past ten years, he has headed the Quantum Device and Terahertz Application Group, IEMN. His current interests concern low-dimensional technology and high-frequency evaluation, micromachining of semiconductor microstructures, and photonic bandgap materials.